

Original Investigation

Neuroanatomy

Step-by-Step Dissection of the Pterygopalatine Fossa, Infratemporal Fossa, and Parapharyngeal Space via the Middle Cranial Fossa Approach with Preservation of the Temporomandibular Joint

Yandong SU¹, Zhao WANG^{2,3}, Hongxiang WANG¹, Juxiang CHEN¹

¹Changhai Hospital, Naval Medical University, Department of Neurosurgery, Shanghai, China

²Central South University, Xiangya Hospital, Department of Neurosurgery, Changsha, China

³The First Affiliated Hospital of Jishou University, Department of Neurosurgery, Jishou, China

Corresponding author: Juxiang CHEN ✉ juxiangchen@smmu.edu.cn

ABSTRACT

AIM: To illustrate the middle cranial fossa (MCF) approach to the pterygopalatine fossa (PPF), infratemporal fossa (ITF), and parapharyngeal space (PPS) with temporomandibular joint (TMJ) preservation through step-by-step cadaver dissection and discuss certain critical considerations that are inadequately addressed in the literature.

MATERIAL and METHODS: Six sides of three formalin-fixed, latex-injected specimens were dissected under an operating microscope to illustrate this unique approach. All steps were documented.

RESULTS: The MCF approach with TMJ preservation provides excellent access to the PPF and ITF, and limited exposure of the PPS. Key steps include positioning and craniotomy, lateral loop drilling, MCF removal, PPF dissection, ITF dissection, maxillary artery dissection, and PPS dissection.

CONCLUSION: The MCF is a promising corridor for accessing these complex exocranial skull base areas. Although live surgery may be quite different from cadaver dissection, every surgeon must master the relevant anatomy before entering the operation theatre.

KEYWORDS: Middle cranial fossa approach, Pterygopalatine fossa, Infratemporal fossa, Parapharyngeal space, Temporomandibular joint preservation

ABBREVIATIONS: ATN: Auriculotemporal nerve, BN: Buccal nerve, CT: Chorda tympani, DTN: Deep temporal nerve, IAN: Inferior alveolar nerve, LN: Lingual nerve, LPM/LPN: Lateral pterygoid muscle/nerve, MCF: Middle cranial fossa, MN: Masseteric nerve, MPM/MPP: Medial pterygoid muscle/plate, ICA: Internal carotid artery, ITF: Infratemporal fossa, PPF: Pterygopalatine fossa, PPG: Pterygopalatine ganglion, PPS: Parapharyngeal space, SML: Sphenomandibular ligament, SPCM: Superior pharyngeal constrictor muscle, TMJ: Temporomandibular joint, TVPM: Tensor veli palatini muscle, VC: Vidian canal, ZN: Zygomatic nerve, V2: Maxillary nerve, V3: Mandibular nerve

Yandong SU : 0009-0008-6143-5418

Zhao WANG : 0000-0003-1148-0276

Hongxiang WANG : 0000-0003-4839-3985

Juxiang CHEN : 0000-0002-5171-9707



This work is licensed by "Creative Commons Attribution-NonCommercial-4.0 International (CC)".

INTRODUCTION

The pterygopalatine fossa (PPF), infratemporal fossa (ITF), and parapharyngeal space (PPS) represent intricate skull base compartments, posing significant challenges for surgical access. Lesions in these areas are managed by various specialists, including neurosurgeons, otorhinolaryngologists, head and neck surgeons, and oral and maxillofacial surgeons. Surgeons from different specialties have proposed diverse approaches based on their individual understanding and customary practices, such as anterior (midfacial degloving, maxillary swing), lateral (mandibulotomy, Sekhar's subtemporal-preauricular ITF), posterolateral (Fisch's ITF approaches types A-C), and inferolateral (submandibular, transcervical) approaches (1-3,15). However, all these approaches result in significant cosmetic deformities and functional disturbances due to incisions in the cervicofacial region and aggressive manipulation of the viscerocranium bones. Even the supposedly less invasive endoscopic transnasal/tranoral approaches, widely accepted over the past two decades, require sacrificing important structures such as the vidian nerve and Eustachian tube (14).

The middle cranial fossa (MCF) serves as the roof for the PPF and ITF while being in close proximity to the PPS, offering a natural corridor for surgical access. The transcranial MCF approach with temporomandibular joint (TMJ) preservation, targeting lesions from the superolateral aspect, is well established (11,12,17). The reported clinical outcomes are quite good, given its excellent surgical exposure and minimal disturbance to normal structures (7,11,12). However, identifying individual structures along this trajectory is more challenging due to its unique orientation. Many surgeons employ this approach in clinical practice, but few possess a thorough understanding of the relevant anatomy. This is understandable, considering that most tumors they handle are benign, well encapsulated, and can be safely resected using extracapsular dissection without the need to distinguish each normal structure in the vicinity. Unfortunately, comprehensive anatomical descriptions of this approach, including step-by-step dissection, are scarce in the literature, and some crucial considerations remain inadequately discussed. Thus, we conducted a cadaveric dissection study to unveil the challenging anatomy and presented our insights for reference.

MATERIAL and METHODS

Three formalin-fixed and latex-injected adult cadaveric heads that were free of known diseases were used. Veins were intentionally excluded from injection for better demonstration of the important anatomical structures. All six unilateral dissections were meticulously performed by a neurosurgeon skilled in head and neck anatomy (Y.S.). Dissections were completed using standard surgical/microsurgical instruments and an operating microscope (Hotry, Beijing, China). All procedure steps were recorded using the high-definition camera and video system integrated into the microscope. Institutional review board approval was not required because this was a cadaveric laboratory study.

RESULTS

Positioning and Craniotomy

The specimen is positioned supine, with the head rotated 70° to the contralateral side and flexed by 15°, and securely fixed in a three-pin skull clamp. A preauricular question-mark-shaped incision is made just anterior to the tragus and 1.5cm below the zygoma. With standard interfascial dissection, the scalp is reflected to reveal the lateral orbital rim, the full length of the zygomatic arch, the TMJ capsule, and the upper part of the masseter muscle. Subsequently, an extended frontotemporal craniotomy and a T-shaped zygomatic osteotomy are performed (Figures 1A, B). Following this, the lateral and superior orbit walls are skeletonized (Figure 1C), and the temporal squama is removed to the level of the MCF. The lateral wall of the cavernous sinus is peeled to facilitate temporal lobe retraction and expose the superior orbital fissure, maxillary nerve (V2), and mandibular nerve (V3) (Figure 1D).

Lateral Loop Drilling

The lateral loop is defined as the curve demarcated by the lateral margin of V2 and the ventral margin of V3 (18). Drilling the bone around the loop to expose the vidian canal (VC), roof of the nasopharynx, and pterygoid fossa is the critical step for this approach.

Once V2 and V3 are fully skeletonized, the lateral loop can be quickly and easily drilled away using large drill bits. The initial structures encountered are either the emissary vein of Vesalius or the mucosa of the lateral recess of the sphenoid sinus (Figure 2A). The former is a venous structure anteromedial to V3, while the latter may not be visible at the early stage unless the sinus is well pneumatized.

Continued drilling exposes the VC, which courses from back to front and has a trumpet-like opening at its anterior end. Drilling below the VC reveals the roof of the nasopharynx medially and the contents of the pterygoid fossa laterally (Figure 2B). The internal carotid artery (ICA) of the lacerum segment can be identified at the posterior end of the VC (Figure 2C).

MCF Removal

The region of the MCF, situated laterally to the sphenosquamosal suture and anterior to the TMJ, is meticulously rongeuired off while preserving all the periosteum encountered at this stage. Subperiosteal dissection towards the medial aspect reveals the lateral pterygoid plate (Figure 2D). Lateral loop drilling becomes significantly easier if MCF removal is performed first.

ITF Dissection

The V3 is exposed through the careful incision of its sheath, followed by tracing the nerve to the ITF. The branches of the anterior trunk of V3, excluding the buccal nerve (BN), are located on the superior aspect of the superior head of the lateral pterygoid muscle (LPM). These branches include the masseteric nerve (MN), deep temporal nerve (DTN), and lateral pterygoid nerve (LPN) from the back to the front (Figure 3A). DTNs may arise from V3 or from the MN and LPN, but the most anterior DTN always originates from the BN. The BN

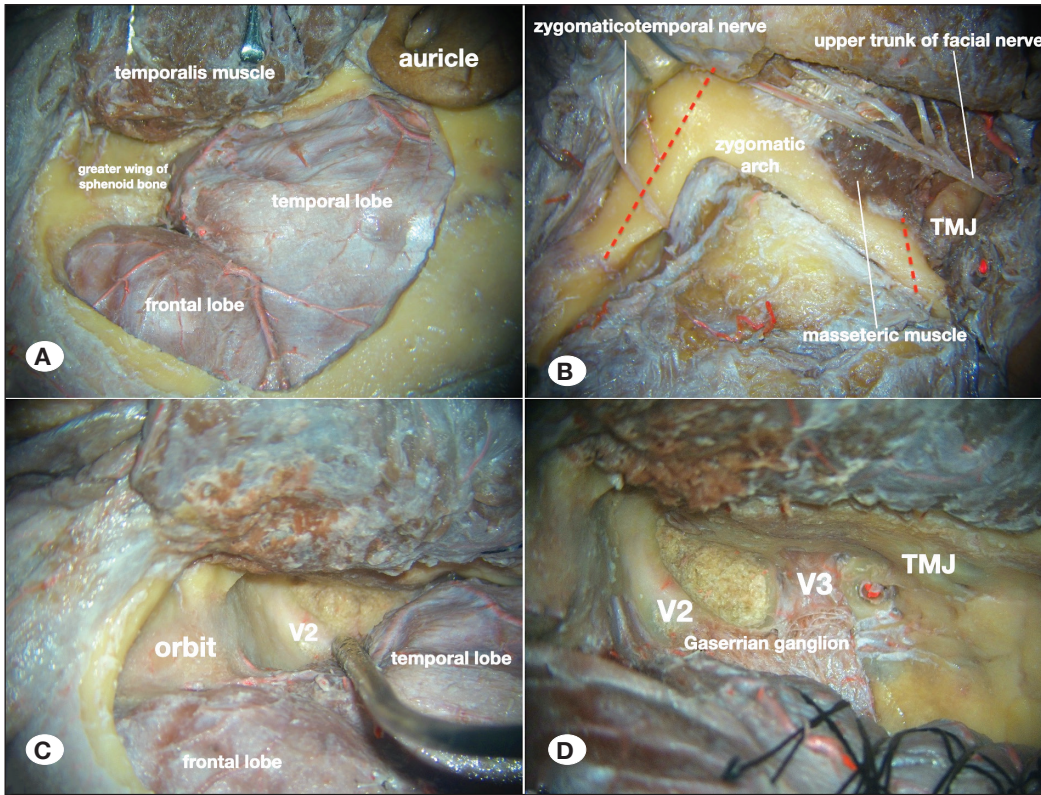


Figure 1: Craniotomy on the right side. **A)** With a preauricular incision, a frontotemporal craniotomy extending at least 2cm posterior to the root of the zygoma is performed. **B)** A T-shaped zygomatic osteotomy is performed, with the posterior cut as close to the articular tubercle as possible, facilitating inferior retraction of the temporalis muscle. **C)** Skeletonization of the orbit is performed. **D)** The temporal squama is rongeuared off until it reaches the middle cranial fossa. The lateral wall of the cavernous sinus is then peeled to expose V2 and V3 for skeletonization. **TMJ:** temporomandibular joint.

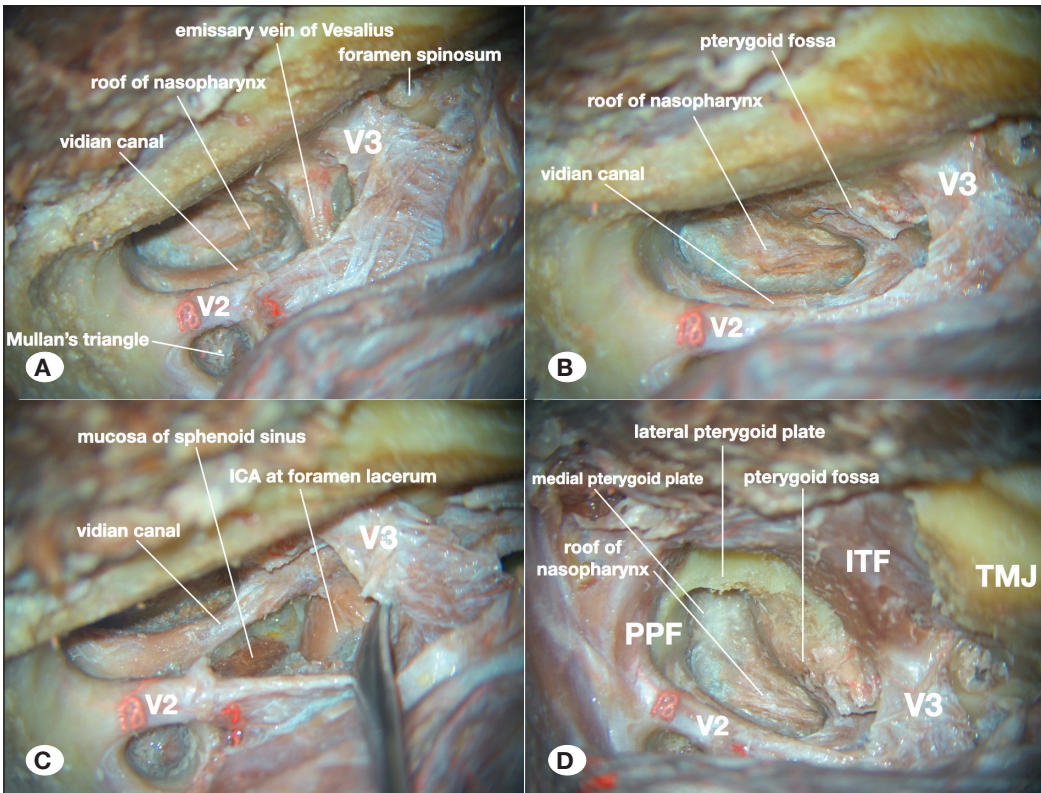


Figure 2: Lateral loop drilling and MCF removal on the right side. **A)** Due to poor sphenoid sinus pneumatization, the emissary vein of Vesalius is encountered first in this case. **B)** This vein is resected to expose the posterior segment of the vidian canal. The roofs of the nasopharynx and pterygoid fossa are accessed inferomedial and inferolateral to the vidian canal, respectively. **C)** The ICA is exposed at the posterior end of the vidian canal, and the mucosa of the sphenoid sinus observed above the canal. **D)** Following MCF removal and subperiosteal dissection, the lateral pterygoid plate becomes visible. **ITF:** Infratemporal fossa, **PPF:** pterygopalatine fossa, **TMJ:** temporomandibular joint.

courses medially to the superior head of the LPM and then anteroinferiorly between the two heads of the LPM. Therefore, the BN serves as a landmark for the resection of the superior head of the LPM, after which the anterior DTN can be dissected (Figure 3B). All branches of the anterior trunk of V3 are currently exposed.

Next, the inferior head of the LPM along with the residual LPNs are resected to identify the lingual nerve (LN) and inferior alveolar nerve (IAN). The fascia covering the medial pterygoid muscle is opened to expose the medial pterygoid nerve, which originates directly from V3 and coursing along the outer surface of the tensor veli palatini muscle (Figure 3C). On the posterior aspect, the auriculotemporal nerve (ATN) is dissected, revealing two separate branches that encircle the middle meningeal artery before merging (Figure 3H). Tracing the LN and IAN inferiorly, the mylohyoid nerve and chorda tympani (CT) are exposed, with the possibility of presence of a communicating branch(es) between the LN and IAN (Figures 3D, E). The CT, located medially to the IAN and ATN, exits the skull base medial to the sphenoid spine and reaches the posterior aspect of the LN (Figure 3E). At this stage, all relevant anatomy of the posterior trunk of V3 is revealed.

The lateral pterygoid plate is removed, followed by resection of the medial pterygoid muscle (including its superficial and deep heads, MPM) to reveal the tensor veli palatini muscle (TVPM) (Figure 3F). The prestyloid space/anterior compartment of the parapharyngeal space, housing the fat tissue, ascending palatine artery, and accompanying veins, is beneath the TVPM. The fat tissue within the space is exenterated to expose the superior pharyngeal constrictor muscle (SPCM) (Figure 3F). The medial pterygoid plate (MPP) lies anteromedial to the TVPM, with its inferior portion (pterygoid hamulus) serving as a trochlea for the TVPM to turn medially and insert into the palatine aponeurosis (Figure 3G). Removing the TVPM uncovers the cartilaginous part of the Eustachian tube with the levator veli palatini muscle on its inferomedial side (Figure 3H).

PPF Dissection

The bone between the V2 and VC is drilled to fully expose the posterior wall of the PPF. Meticulous opening of the V2 sheath beginning from the proximal segment facilitates the dissection of main branches of V2, including the zygomatic nerve (ZN), posterior superior alveolar nerve, and infraorbital nerve (Figure 4A). The ZN is often adherent to the V2 sheath, posing a high risk of injury during dissection. It has an anterior and slightly superior orientation, coursing between the orbitalis muscle of Müller and the periorbita. Sometimes, the ZN departs from V2 very early and can be visualized through the transparent periorbita.

After the opening of the VC and posterior wall of the PPF, the vidian nerve is identified and followed anteriorly to the pterygopalatine ganglion (PPG) (Figure 4B). Then, the communicating branches between V2 and PPG are carefully dissected. Inferior traction along the PPG reveals the greater and lesser palatine nerves in their respective canals (Figure 4C). The final step of this section involves removing fat tissue

within the PPF by laterally transposing V2 to expose the nasopalatine nerve and palatovaginal nerve emerging from the medial aspect of the PPG (Figure 4D).

Maxillary Artery Dissection

Finding the proximal maxillary artery is challenging, but once the infraorbital nerve and pterygopalatine ganglion are identified, the infraorbital artery and sphenopalatine artery can be easily exposed simultaneously. Therefore, the distal-to-proximal technique is the best way to free the maxillary artery. Moreover, during the procedure of maxillary artery isolation, the residual LPM can be identified and removed, which creates more space for the subsequent PPS dissection.

PPS Dissection

In this section, the first step involves removing the fat tissue medial and posterior to the LN/IAN, exposing the sphenomandibular ligament (SML), a fibrous band connecting the sphenoid spine and mandibular lingula. Dissecting through the corridor formed by the LN/IAN anteriorly and the SML posteriorly, the styloid diaphragm is reached and confirmed by palpating the rigid styloid process (SP) with a dissector (Figure 5A). Next, the diaphragm is incised and reflected anteriorly. The styloglossus and stylopharyngeus muscles are observed attaching to the anterior and medial surfaces of the SP, respectively (Figure 5B). Exposing the stylohyoid muscle is not easy due to the narrow working corridor. The parapharyngeal ICA is located on the anteromedial side of the SP, and lymph node(s) may present around the artery (Figure 5B). The glossopharyngeal nerve runs anteroinferiorly, and is located between the ICA and stylopharyngeus muscle (Figure 5C, D). Finally, the ascending pharyngeal artery is exposed on the medial side of the ICA (Figure 5D).

DISCUSSION

The MCF approach offers excellent access to the PPF and ITF while providing limited exposure to the PPS, especially the retrostyloid space. This procedure is highly complex and demands advanced techniques. Before conducting this approach, several critical considerations should be addressed.

Vulnerable Structures

Dissection of the ITF and PPS primarily occurs within the corridor defined by the buccal nerve anteriorly and the masseteric nerve posteriorly (Figure 3C, 5D). The superficial structures within this corridor include the deep temporal nerves and lateral pterygoid nerves, and preservation of these nerves is always impossible. Moreover, there is a high risk of interruption of the buccal and masseteric nerves if they are not adequately freed. However, in the clinical setting, many patients indicated for this approach already present preoperative wasting of the mastication muscles due to a V3 deficit, (8) making nerve injury a minor concern.

Exposing the entire zygomatic arch necessitates a skin incision below the zygoma, posing the potential risk of damaging the temporal branches of the facial nerve. Given the uncertain courses of these branches, our standard practice involves

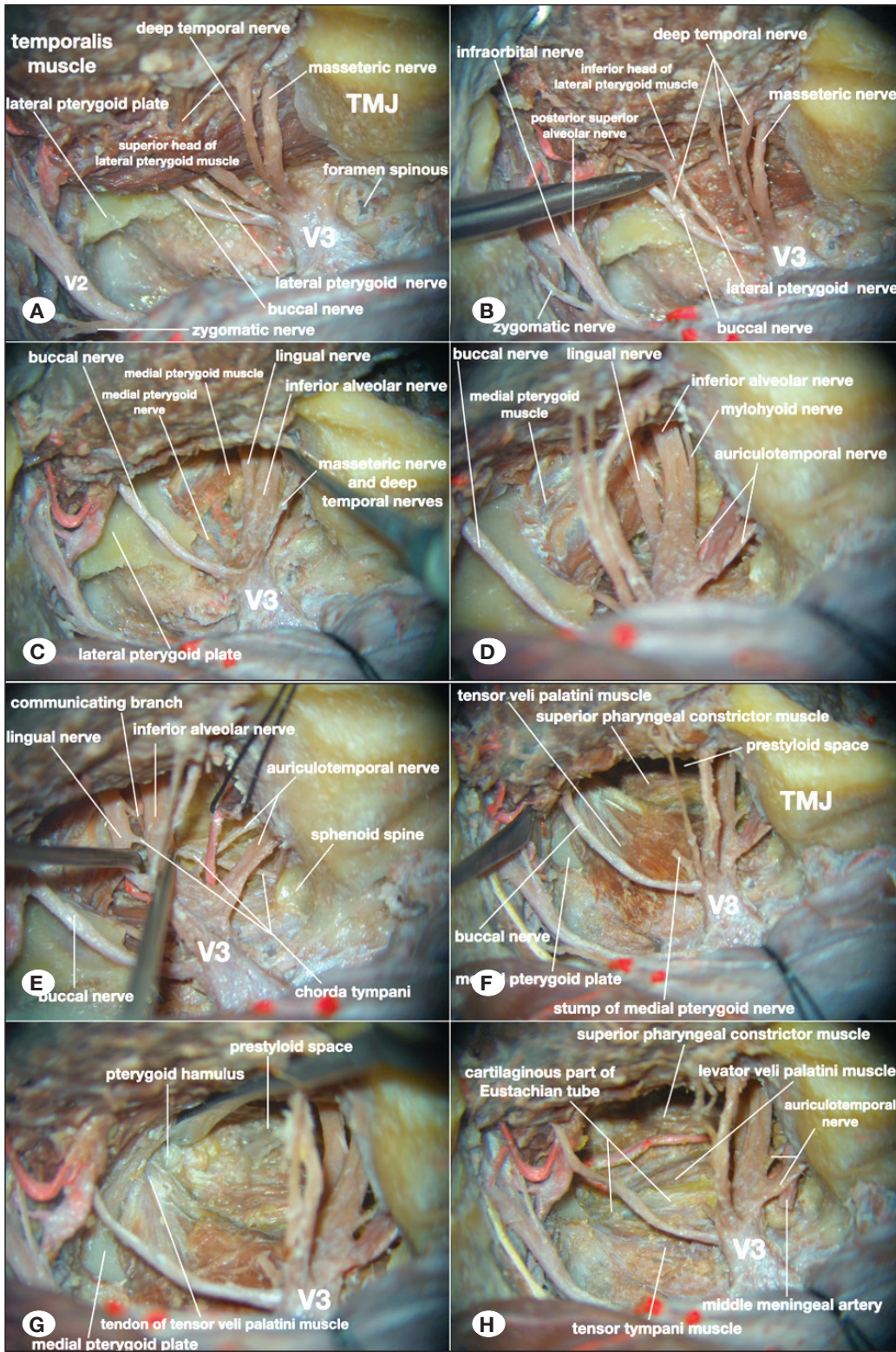


Figure 3: ITF dissection on the right side. **A)** The branches of the anterior trunk of V3 are exposed when the exocranial MCF periosteum is removed. **B)** Resection of the superior head of the lateral pterygoid muscle shows that the anterior deep temporal nerve arises from the buccal nerve. **C)** The inferior head of the lateral pterygoid muscle is removed to expose the lingual and inferior alveolar nerves running inferiorly along the lateral aspect of the medial pterygoid muscle. The medial pterygoid nerve is found anterior to these two nerves in a deeper plane. **D)** Following the inferior alveolar nerve, the mylohyoid nerve is identified. **E)** The foramen spinosum is completely drilled away, and the auriculotemporal nerve is dissected. The entire extratemporal course of the chorda tympani is visible, along with a small branch connecting the lingual nerve and inferior alveolar nerve. **F)** Full exposure of the tensor veli palatini muscle is achieved by removing the lateral pterygoid plate and medial pterygoid muscle. Clearing the fat tissue in the prestyloid space reveals the superior pharyngeal constrictor muscle. **G)** Behind the medial pterygoid plate, the tensor veli palatini muscle converges anteroinferiorly, with its tendon turning medially at the pterygoid hamulus to form the palatine aponeurosis. **H)** Resecting the tensor veli palatini muscle exposes the cartilaginous part of the Eustachian tube, along with the levator veli palatini muscle on its inferomedial side. **TMJ:** Temporomandibular joint.

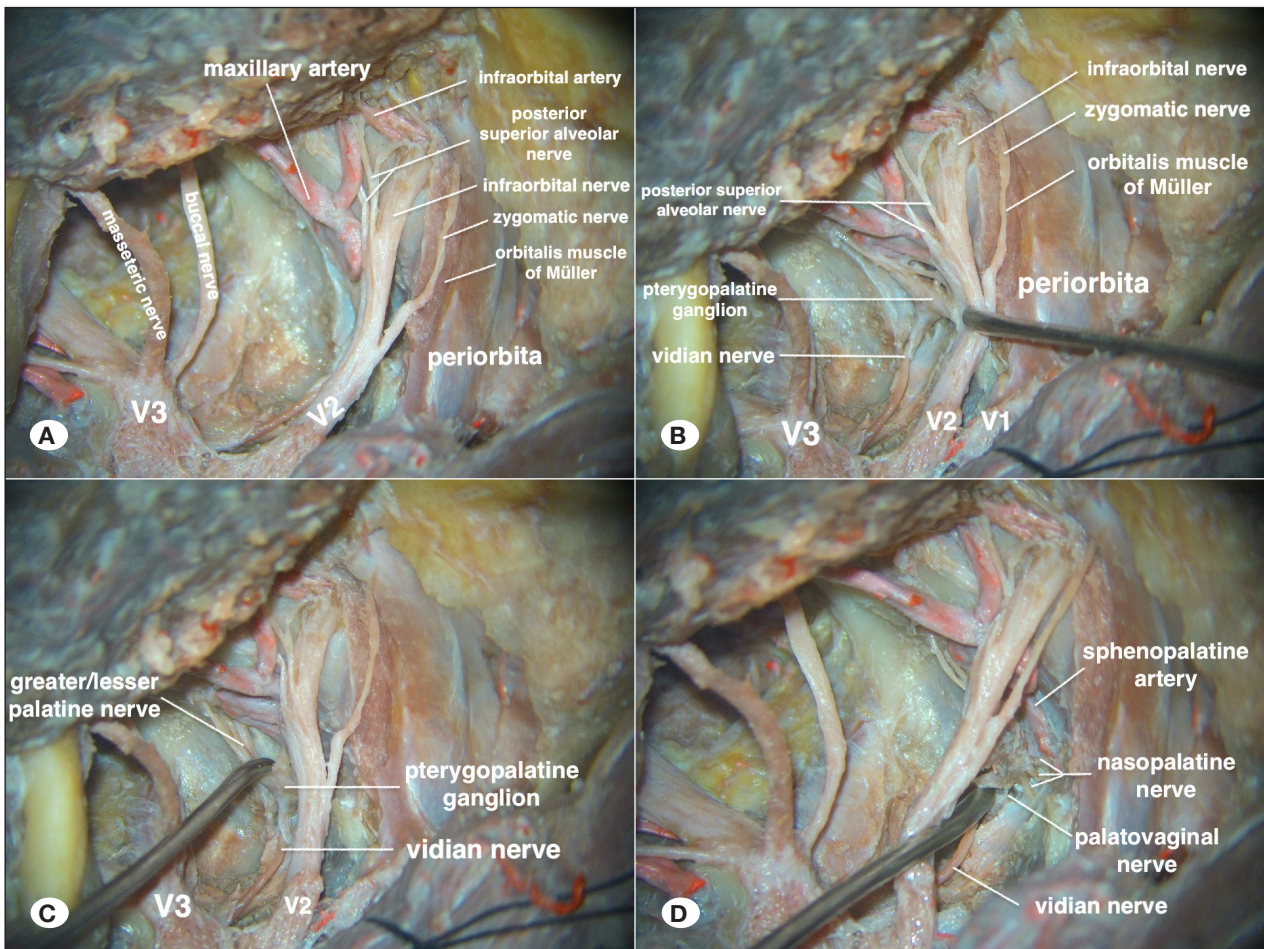


Figure 4: PPF dissection on the left side. **A)** The V2 sheath is opened and followed to the zygomatic, infraorbital, and posterior superior alveolar nerves. The zygomatic nerve runs anteriorly and superiorly between the periorbita and orbitalis muscle of Müller. The infraorbital artery can be found adjacent to the namesake nerve and traced back to the distal segment of the maxillary artery. **B)** Upon removing the posterior wall of the PPF, the pterygopalatine ganglion is identified as the anterior attachment of the vidian nerve. **C)** The greater and lesser palatine nerves emerge as a bundle from the inferior aspect of the pterygopalatine ganglion, which then divides into individual nerves that enter their respective canals. **D)** The nasopalatine and tiny palatovaginal nerves are exposed on the medial aspect of the pterygopalatine ganglion after removing the fat tissue within the PPF. The sphenopalatine artery is identified simultaneously.

placing the incision as close to the tragus as possible, thereby preserving the main trunk of the superficial temporal artery simultaneously. Another consideration is that an incision with a more inferior extension may be required in obese patients, carrying the risk of injuring the temporofacial trunk of the facial nerve. In such cases, we recommend reflecting the skin flap beneath the masseteric fascia and dissecting along the cartilage of the external ear canal to protect the entire parotid gland.

Extensions of the Current Approach

MCF serves as a versatile corridor. Building upon the basic approach outlined in the *Results* section, its extensions enable the targeting of other anatomical areas. Moreover, the introduction of an endoscope significantly enhances exposure (20).

Guided by the PPF, the nasal cavity and paranasal sinuses become readily accessible, particularly with the concurrent use of an endoscope (13,19). Resection of the cartilaginous portion of the Eustachian tube and levator veli palatini muscle exposes the nasopharynx, revealing the soft palate, oropharynx, and retropharyngeal space (Figure 6B-D). Furthermore, an incision in the pterygomandibular raphe directs the surgeon to the oral cavity (Figure 6A).

The combination of temporal bone drilling enhances the exposure of the internal carotid artery (ICA) and clivus. Removal of the tegmen tympanum, bony part of the Eustachian tube, tensor tympani muscle, and vaginal process reveals the petrous ICA, providing exposure from the parapharyngeal segment to the lacerum segment (Figures 7A-D). Identification of the petroclival fissure, covered by dense fibrous tissue, enables clivectomy. Additionally, mastoid drilling can be performed as required (Figure 7E, F) (6).

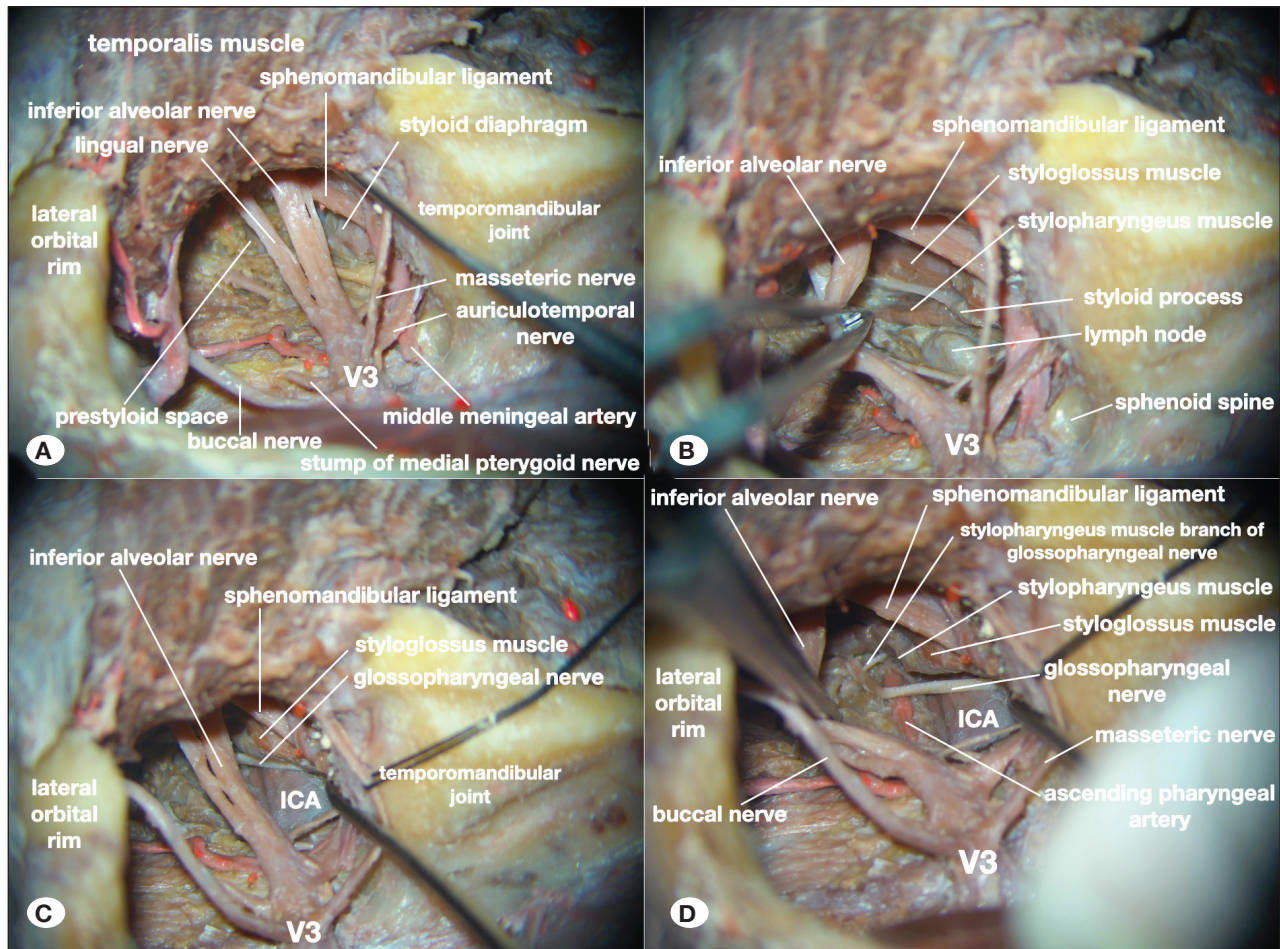


Figure 5: PPS dissection on the right side. **A)** The fat tissue behind the V3 is removed to expose the sphenomandibular ligament. Access to the styloid diaphragm is obtained between this ligament and V3. **B)** Opening the styloid diaphragm covering the styloid process exposes the styloglossus and stylopharyngeus muscles. Note the lymph node on the surface of ICA. **C)** After removing the lymph node, the ICA appears anteromedial to the styloid process. **D)** The glossopharyngeal nerve and its branch innervating the stylopharyngeus muscle are located between this muscle and ICA. The ascending pharyngeal artery usually runs upwards, medial to the ICA.

Resecting the styloid process and its apparatus to expose the structures lateral and posterior to the parapharyngeal ICA is a viable option. In clinical practice, when such exposure becomes necessary, the posterolateral ITF approach is recommended due to its superior control of the ICA, as opposed to the current approach (11).

Intraoperative Challenges

During live surgery, several critical issues must be addressed, with the most prominent being brain relaxation and control of venous bleeding. This is a downwards-looking procedure. Although zygomatic osteotomy with maximal inferior reflection of the temporalis muscle is performed to achieve basal exposure, retraction of the temporal lobe remains needed. Strategies to address this challenge involve facilitating the retraction and/or reducing the retraction requirement. The former includes utilizing lumbar drainage and ensuring well-conducted anesthesia, while the latter is primarily achieved through the introduction of an endoscope (20).

Enormous venous bleeding from the pterygoid plexus, a large venous confluence that collects blood flow from the cavernous sinus, nasal cavity/paranasal sinuses, and infratemporal fossa, may be encountered. Preserving the fascia enveloping the plexus by dissecting along the true tumor capsule and packing gauzes/neuropatties within the dissecting plane can prevent hemorrhage (10,22). In the event of bleeding, hemostatic materials are applied in a manner similar to that used for cavernous sinus hemostasis. However, it is crucial to note that the pterygoid plexus encompasses the V3 and the maxillary artery along with its branches. Therefore, any active arterial bleeding should be stopped by coagulation beforehand.

Certainly, ICA injury should be a major concern. However, we believe that with sufficient exposure and a clean surgical field, the ICA can be easily identified and controlled, leading to minimal risk of injury (6).

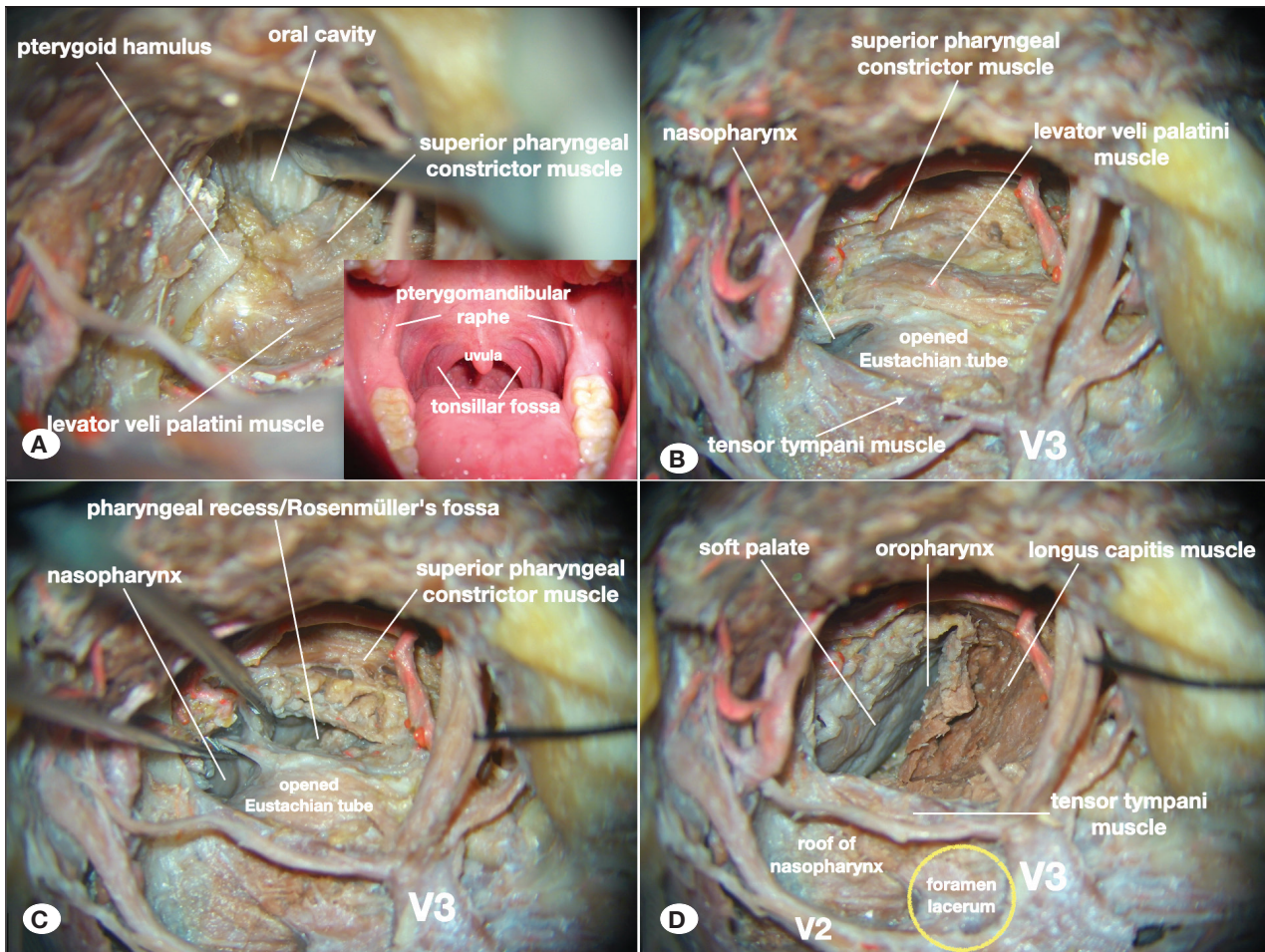


Figure 6: Nasopharyngeal and oropharyngeal extensions on the right side. **A)** Access to the oral cavity is achieved by incising the pterygomandibular raphe, extending inferolaterally from the pterygoid hamulus and serving as the attachments of the buccinator muscle and superior pharyngeal constrictor muscle. The insert displays the raphe as observed from the oral cavity of a living person. **B)** Resection of the lateral wall of the cartilaginous part of the Eustachian tube illustrates its nasopharyngeal opening. **C)** Following the removal of the levator veli palatini muscle and a portion of the pharyngobasilar fascia, the pharyngeal recess is exposed. **D)** Lateral nasopharyngectomy is completed by resecting the residual cartilaginous Eustachian tube, exposing the soft palate, oropharynx, and retropharyngeal space. Additionally, the longus capitis muscle in the posterior wall of the oropharynx becomes visible.

CSF Leak Prevention/Reconstruction

Understanding the pathway(s) of CSF leakage is crucial because it guides the selection of different reconstructive strategies. In the basic approach, CSF escapes through the opened sphenoid sinus and air cells around the root of the zygoma. At the conclusion of the surgery, if the dura remains intact, only sealing the temporal squama with bone wax and closing the sphenoid sinus with a fat/muscle graft are necessary. If not, in addition to the aforementioned methods, achieving a watertight closure of the dura is attempted. Subsequently, vascularized flap(s) (fascia and/or muscle), which act as the most reliable barrier against the leakage, are utilized to isolate the cranial cavity from the exocranial compartment (4,9).

Nevertheless, in the extended approaches, the opening of the nasal cavity/paranasal sinuses, Eustachian tube, and

naso-/oropharynx may induce more leakage pathways. The key considerations for successful reconstruction involve filling the entire dead space created by exposure and tumor removal with a fat graft or muscle, with or without a pedicle. Additionally, vascularized flap(s) are used to cover the entire MCF defect. Eustachian tube opening always accompanies petrous bone drilling and middle ear unveiling for ICA control. In this scenario, the tube should be occluded, and the temporal bone cavity be waxed and packed. Reconstruction following the division of the naso-/oropharynx is complex. Repair strategies include primary closure if there is minimal risk of postoperative stenosis and other complications; otherwise, the use of a free myocutaneous flap or pedicle flap (e.g., the temporalis muscle, submental flap, fascias of the scalp, and nasoseptal mucosal flap harvested through an additional transnasal approach) is considered (5,16,21).

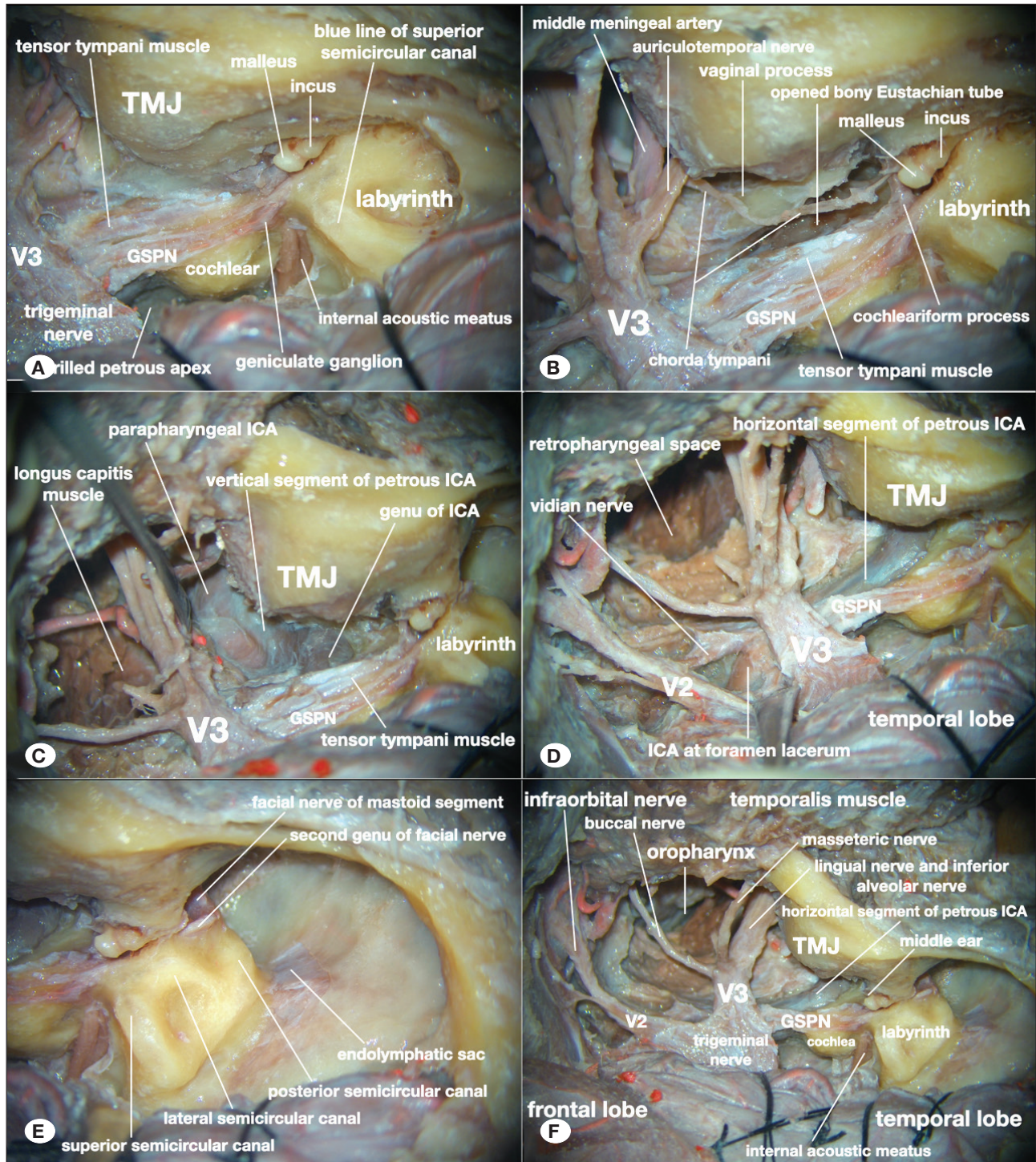


Figure 7: Temporal bone extension on the right side. **A)** Initiated by meticulous skeletonization of the blue line of the superior semicircular canal, maximal anterior petrosectomy is performed. Removing the tegmen tympanum and tegmen mastoideum unveils the ossicular chain and labyrinth. The MCF covering the tensor tympani muscle is also drilled. **B)** The residual greater wing of the sphenoid bone, i.e., the sphenoid spine, is removed, and the chorda tympani is carefully dissected out. Subsequently, the bony part of Eustachian tube is opened. **C)** The chorda tympani is transected and the vaginal process of the tympanic bone is drilled away to reveal the vertical segment of the petrous ICA. **D)** The entire tensor tympani muscle is resected to expose the horizontal segment of the petrous ICA, which is better visualized by drilling the petrous bone lateral and inferior to the artery. **E)** The craniotomy is expanded on the posterior aspect to allow sufficient working space for mastoid drilling. It is crucial to identify the blue lines of the three semicircular canals for safe labyrinthine skeletonization. This trajectory provides exposure to most structures within the mastoid process. **F)** Overview of the final dissection. **GSPN:** Greater superficial petrosal nerve, **TMJ:** temporomandibular joint.

CONCLUSION

The MCF approach is a promising route to the PPF, ITF and PPS. In live surgery, the tumor can be removed with “tumor corridor” and extracapsular dissection techniques. Therefore, it may be unnecessary to dissect the surrounding tissues, but what structures are nearby should always be in the surgeons’ mind. It is mandatory for every surgeon to master this anatomy before entering the operating theatre.

ACKNOWLEDGMENTS

The author (Y.S.) gratefully acknowledges the encouragement and guidance received from Professor Atul Goel. The authors express gratitude to Hotry Company (Beijing, China) for providing the necessary setup for cadaver dissections, and to Dr. Deborah Oluwatosin Fasoranti from Xiangya Hospital, Changsha, China, for her English editing service.

Sincere appreciation is extended to those who generously donated their bodies to science; both the donors and their families deserve our highest gratitude.

Supplementary information: The author, Yandong Su, M.D., has conducted a live dissection of this unique approach, which can be watched at <https://www.youtube.com/watch?v=Mfk-fkLaCta0>.

Declarations

Funding: None

Availability of data and materials: The datasets generated and/or analyzed during the current study are available from the corresponding author by reasonable request.

Disclosure: The authors declare no competing interests.

Ethics approval: Institutional review board approval was not required because this was a cadaveric laboratory study.

AUTHORSHIP CONTRIBUTION

Study conception and design: YS, JC

Data collection: YS, ZW

Analysis and interpretation of results: YS

Draft manuscript preparation: YS

Critical revision of the article: YS, HW, JC

Other (study supervision, fundings, materials, etc...): YS, JC

All authors (YS, ZW, HW, JC) reviewed the results and approved the final version of the manuscript.

REFERENCES

- Dwivedi G, Gupta V, Tiwari V, Patnaik U, Sood A, Kumari A, Bharadwaja S: Different approaches to the overlapping infratemporal fossa and parapharyngeal spaces: a case series and review of literature. *Indian J Otolaryngol Head Neck Surg* 74:2337-2343, 2022. <https://doi.org/10.1007/s12070-020-02168-2>
- Fisch U: The infratemporal fossa approach for nasopharyngeal tumors. *Laryngoscope* 93:36-44, 1983. <https://doi.org/10.1288/00005537-198301000-00007>
- Fisch U, Fagan P, Valavanis A: The infratemporal fossa approach for the lateral skull base. *Otolaryngol Clin North Am* 17:513-552, 1984
- Gagliardi F, Piloni M, Bailo M, Gragnaniello C, Nocera G, Boari N, Spina A, Caputy AJ, Mortini P: Temporal myofascial segmentation for multilayer reconstruction of middle cranial fossa floor after extradural subtemporal approach to the clival and paraclival region. *Head Neck* 41:3631-3638, 2019. <https://doi.org/10.1002/hed.25896>
- Gan JY, Yeo MSW, Fu EWZ, Tan NC, Lim MY: Reconstruction of nasopharynx defect using a free flap after endoscopic nasopharyngectomy-feasibility and technical considerations. *JAMA Otolaryngol Head Neck Surg* 2020 (Online ahead of print). <https://doi.org/10.1001/jamaoto.2020.2187>
- Goel A: Middle fossa sub-Gasserian ganglion approach to clivus chordomas. *Acta Neurochir* 136:212-216, 1995. <https://doi.org/10.1007/BF01410628>
- Goel A, Nadkarni T: Basal lateral subtemporal approach for trigeminal neurinomas: Report of an experience with 18 cases. *Acta Neurochir (Wien)* 141:711-719, 1999. <https://doi.org/10.1007/s007010050366>
- Goel A, Shah A, Muzumdar D, Nadkarni T, Chagla A: Trigeminal neurinomas with extracranial extension: Analysis of 28 surgically treated cases. *J Neurosurg* 113:1079-1084, 2010. <https://doi.org/10.3171/2009.10.JNS091149>
- Kusumi M, Fukushima T, Mehta AI, Cunningham CD, 3rd, Friedman AH, Fujii K: Middle fossa approach for total resection of petrous apex cholesterol granulomas: Use of vascularized galeofascial flap preventing recurrence. *Neurosurgery* 72:77-86; discussion 86, 2013. <https://doi.org/10.1227/NEU.0b013e3182724354>
- Li L, London NR Jr, Prevedello DM, Carrau RL: Anatomical variations and relationships of the infratemporal fossa: Foundation of a novel endonasal approach to the foramen ovale. *J Neurol Surg B Skull Base* 82:668-674, 2021. <https://doi.org/10.1055/s-0040-1715815>
- Nonaka Y, Fukushima T, Watanabe K, Sakai J, Friedman AH, Zomorodi AR: Middle infratemporal fossa less invasive approach for radical resection of parapharyngeal tumors: surgical microanatomy and clinical application. *Neurosurg Rev* 39:87-96; discussion 96-87, 2016. <https://doi.org/10.1007/s10143-015-0655-x>
- Ohue S, Fukushima T, Kumon Y, Ohnishi T, Friedman AH: Preauricular transzygomatic anterior infratemporal fossa approach for tumors in or around infratemporal fossa lesions. *Neurosurg Rev* 35:583-592; discussion 592, 2012. <https://doi.org/10.1007/s10143-012-0389-y>
- Oyama K, Watanabe K, Hanakita S, Champagne PO, Passeri T, Voormolen EH, Bernat AL, Penet N, Fukushima T, Froelich S: The orbitopterygoid corridor as a deep keyhole for endoscopic access to the paranasal sinuses and clivus. *J Neurosurg* 134:1480-1489, 2020. <https://doi.org/10.3171/2020.3.JNS2022>

14. Rivera-Serrano CM, Terre-Falcon R, Fernandez-Miranda J, Prevedello D, Snyderman CH, Gardner P, Kassam A, Carrau RL: Endoscopic endonasal dissection of the pterygopalatine fossa, infratemporal fossa, and post-styloid compartment. Anatomical relationships and importance of eustachian tube in the endoscopic skull base surgery. *Laryngoscope* 120 Suppl 4:S244, 2010. <https://doi.org/10.1002/lary.21711>
15. Sekhar LN, Schramm VL Jr, Jones NF: Subtemporal-preauricular infratemporal fossa approach to large lateral and posterior cranial base neoplasms. *J Neurosurg* 67:488-499, 1987. <https://doi.org/10.3171/jns.1987.67.4.0488>
16. Sun X, Liu Q, Yu H, Wang H, Zhao W, Gu Y, Li H, Zhao K, Song X, Wang D, Miranda JCF, Snyderman CH: Transinfratemporal fossa transposition of the temporalis muscle flap for skull base reconstruction after endoscopic expanded nasopharyngectomy: Anatomical study and clinical application. *J Neurol Surg B Skull Base* 83:159-166, 2022. <https://doi.org/10.1055/s-0040-1718764>
17. Vilela MD, Rostomily RC: Temporomandibular joint-preserving preauricular subtemporal-infratemporal fossa approach: Surgical technique and clinical application. *Neurosurgery* 55:143-153; discussion 153-154, 2004. <https://doi.org/10.1227/01.neu.0000126939.20441.dc>
18. Wanibuchi M, Murakami G, Yamashita T, Minamida Y, Fukushima T, Friedman AH, Fujimiya M, Houkin K: Midsubtemporal ridge as a predictor of the lateral loop formed by the maxillary nerve and mandibular nerve: A cadaveric morphological study. *Neurosurgery* 69:ons95-98; discussion ons98, 2011. <https://doi.org/10.1227/NEU.0b013e31821247f5>
19. Watanabe K, Passeri T, Hanakita S, Giammattei L, Zomorodi AR, Fava A, Abbritti R, Labidi M, Champagne PO, Fukushima T, Froelich S: Extradural anterior temporal fossa approach to the paranasal sinuses, nasal cavities through the anterolateral and anteromedial triangles: Combined microscopic and endoscopic strategy. *Acta Neurochir (Wien)* 163:2165-2175, 2021. <https://doi.org/10.1007/s00701-021-04850-y>
20. Yacoub A, Schneider D, Ali A, Wimmer W, Caversaccio M, Anschuetz L: Endoscopic-assisted lateral corridor to the infratemporal fossa: proposal and quantitative comparison to the endoscopic transpterygoid approach. *J Neurol Surg B Skull Base* 82:357-364, 2021. <https://doi.org/10.1055/s-0039-3399553>
21. Yang L, Wang DH: Application of pedicle nasoseptal flap in endoscopic nasopharyngectomy for recurrent nasopharyngeal carcinoma: an analysis of 39 cases. *Zhonghua Er Bi Yan Hou Tou Jing Wai Ke Za Zhi* 57:1212-1218, 2022. <https://doi.org/10.3760/cma.j.cn115330-20210815-00550>
22. Zhou B, Huang Q, Shen PH, Cui SJ, Wang CS, Li YC, Yu ZK, Chen XH, Ye T: The intranasal endoscopic removal of schwannoma of the pterygopalatine and infratemporal fossae via the prelacrima recess approach. *J Neurosurg* 124:1068-1073, 2016. <https://doi.org/10.3171/2015.3.JNS132702>